

# Formation of Supermassive Black Holes in Galactic Bulges: A Rotating Collapse Model Consistent with the $M_{\text{bh}} - \sigma$ Relation

Fred C. Adams<sup>1,2</sup>, David S. Graff<sup>2,3</sup>, Manasse Mbonye<sup>1</sup>, and Douglas O. Richstone<sup>1,2</sup>

<sup>1</sup>*Michigan Center for Theoretical Physics*

*Physics Department, University of Michigan, Ann Arbor, MI 48109*

<sup>2</sup>*Astronomy Department, University of Michigan, Ann Arbor, MI 48109*

<sup>3</sup>*Department of Math and Science*

*United States Merchant Marine Academy, Kings Point, NY 11024*

*DRAFT: 6 March 2003*

## ABSTRACT

Motivated by the observed correlation between black hole masses  $M_{\text{bh}}$  and the velocity dispersion  $\sigma$  of host galaxies, we develop a theoretical model of black hole formation in galactic bulges (this paper generalizes an earlier ApJ Letter). The model assumes an initial state specified by a uniform rotation rate  $\Omega$  and a density distribution of the form  $\rho = a_{\text{eff}}^2/2\pi Gr^2$  (so that  $a_{\text{eff}}$  is an effective transport speed). The black hole mass is determined when the centrifugal radius of the collapse flow exceeds the capture radius of the central black hole (for Schwarzschild geometry). This model reproduces the observed correlation between the estimated black hole masses and the velocity dispersions of galactic bulges, i.e.,  $M_{\text{bh}} \approx 10^8 M_{\odot} (\sigma/200 \text{ km s}^{-1})^4$ , where  $\sigma = \sqrt{2}a_{\text{eff}}$ . To obtain this normalization, the rotation rate  $\Omega \approx 2 \times 10^{15}$  rad/s. The model also defines a bulge mass scale  $M_B$ . If we identify the scale  $M_B$  with the bulge mass, the model determines the ratio  $\mu_B$  of black hole mass to the host mass:  $\mu_B \approx 0.0024 (\sigma/200 \text{ km s}^{-1})$ , again in reasonable agreement with observed values. In this scenario, supermassive black holes form quickly (in  $\sim 10^5$  yr) and are born rapidly rotating (with  $a/M \sim 0.9$ ). This paper also shows how these results depend on the assumed initial conditions; the most important quantity is the initial distribution of specific angular momentum in the pre-collapse state.

*Subject headings:* black hole physics – galaxies: nuclei – galaxies: kinematics and dynamics

## 1. INTRODUCTION

During the past decade, the observational evidence for massive black holes has crossed a threshold of reliability and black holes are now considered to be discovered. Almost every galaxy

is thought to harbor a supermassive black hole anchoring its center (e.g., Magorrian et al. 1998; Kormendy & Richstone 1995). Our own Milky Way galaxy contains a modest central black hole, with its mass estimated at  $M_{\text{mw}} \approx 3 \times 10^6 M_{\odot}$  (e.g., Genzel et al. 1996, Ghez et al. 1998). The properties of these black holes and their connections to their galactic hosts are currently the subject of intensive investigation.

A striking aspect of the black hole-galaxy connection has been recently reported. Two competing groups have observed a relationship between the velocity dispersion  $\sigma$  of the host galaxy and the mass  $M_{\text{bh}}$  of its central (supermassive) black hole (Gebhardt et al. 2000; Ferrarese & Merritt 2000). This correlation can be written in the form

$$M_{\text{bh}} = M_0 (\sigma/200 \text{ km s}^{-1})^{\gamma}, \quad (1)$$

where the two observational teams find slightly different values for the constants in this scaling relation. The exact values derived from the data depend on the fitting procedure and are sensitive to the exclusion of outlying points (see Merritt & Ferrarese 2000, 2001). A recent in-depth analysis (Tremaine et al. 2002) finds that  $\gamma = 4.02 \pm 0.32$  with a mass scale  $M_0 = 1.3 \times 10^8 M_{\odot}$ . In any case, the observed correlation is remarkably tight: The observed scatter in black hole mass  $M_{\text{bh}}$  at fixed dispersion  $\sigma$  is less than 0.30 dex (about a factor of 2). Furthermore, the observed relation appears to be independent of the Hubble type, profile type, or galactic environment. Previous observational surveys have found correlations between the black hole mass and bulge luminosity (Richstone et al. 1998; Magorrian et al. 1998; van der Marel 2000; Kormendy & Richstone 1995; see also Carollo, Stiavelli, & Mark 1998), but the relation [1] appears to be far more robust. This observed scaling relationship provides an important constraint on theories of galaxy formation and bulge formation. Such theories must ultimately account for the production of supermassive black holes at galactic centers and the observed relationship between black hole mass and galactic velocity dispersion.

In a previous paper (Adams, Graff, & Richstone 2001; hereafter Paper I), we presented a theoretical model for black hole formation during the collapse and formation of galactic bulges. This model uses an idealized treatment to describe the collapse of the inner part of protogalaxies. The initial state is assumed to have a density distribution of the form  $\rho \propto r^{-2}$  (like that of a singular isothermal sphere) and a uniform rotation rate; the initial conditions are characterized by an effective transport speed  $a_{\text{eff}}$  and the rotation rate  $\Omega$ . As the collapse develops, material falls inward from ever larger starting radii and carries larger amounts of specific angular momentum. The black hole mass is determined when the centrifugal radius of this collapse flow exceeds the capture radius of the black hole growing at the center. In spite of its idealized nature, this simple model correctly accounts for the observed  $M_{\text{bh}} - \sigma$  relation (equation [1]) with no free adjustable parameters and also predicts the observed ratios of black hole mass to the host (bulge) mass scale. Because of this preliminary success, the model deserves further exploration, which is the subject of this present work.

We note that many other theoretical models have been developed to explain the observed relationship between hole mass and galactic velocity dispersion (e.g., see the recent review of Richstone

2002). A semi-analytic model of merger-driven starbursts with black hole accretion (Haehnelt & Kauffman 2000; Kauffman & Haehnelt 2000) provides a correlation of the observed form (with the proper choice of the free model parameters). Several models are based on the idea that black hole accretion can influence star formation and gas dynamics in the host galaxy; this feedback can occur through ionization, mechanical work, and heating (e.g., Ciotti & Ostriker 1997, 2001; Blandford 1999; Silk & Rees 1998). The model of Blandford (1999) predicts that  $M_{\text{bh}} < \eta \sigma^5$  whereas the model of Silk & Rees (1998) implies  $M_{\text{bh}} \propto \sigma^5$ . The idea that the black hole mass is limited by disk accretion has been explored by Burkert & Silk (2001). Before the observational correlation was discovered, Daniel & Loeb (1995) argued that the seeds for quasar black holes could originate from the collapse of low angular momentum regions. Finally, the accretion of collisional dark matter indicates a scaling relation of the form  $M_{\text{bh}} \propto \sigma^{4-4.5}$  (Ostriker 2000).

This paper is organized as follows. In §2, we review and extend the model presented in Paper I, and describe the orbital infall solutions in greater detail; we also generalize the model to include continued infall onto the black hole at late times. In §3, we consider mass accumulation onto the black hole through disk accretion, more general initial conditions, the effects of mergers, and nonzero quadrupole moments in the initial conditions. We conclude, in §4, with a summary and discussion of our results.

## 2. THE ROTATING COLLAPSE MODEL

In this section, we review and expand upon the basic model of black hole formation during the collapse of a forming galaxy (see Paper I). In this context, we examine the collapse of the inner part of a region that will ultimately form the bulge of a galaxy.

### 2.1. Initial Conditions

The calculation starts at the time of maximum expansion for the main body of the bulge. The main characteristics of the model can be summarized as follows:

[1] All of the matter participating in the collapse – including baryons, dark matter, and stars – are unsegregated. In particular, we assume that all of the collapsing matter has the same initial distribution of specific angular momentum, as this distribution is the key ingredient in producing black holes with the observed properties. However, this model does allow for the possibility that additional material, perhaps some of the dark matter, does not participate in the collapse (see below for further discussion).

[2] The mass and density distributions in this region take the form of a singular isothermal sphere even though the system is not in virial equilibrium. More specifically, the initial density and

mass distributions are assumed to have the form

$$\rho(r) = \frac{a_{\text{eff}}^2}{2\pi Gr^2} \quad \text{and} \quad M(r) = \frac{2a_{\text{eff}}^2}{G} r. \quad (2)$$

The effective transport speed  $a_{\text{eff}}$  that specifies the initial conditions is related to the isotropic velocity dispersion  $\sigma$  according to  $\sigma = \sqrt{2}a_{\text{eff}}$ , where  $\sigma$  is the velocity dispersion of the final state. This relation results from converting half of the original potential energy into kinetic energy, with the overall radius of the structure shrinking by a factor of 2 (see also below). For gaseous material, the transport speed  $a_{\text{eff}}$  plays the role of the sound speed. For any dark matter participating in the collapse, the intrinsic velocity distribution of its initial state is highly ordered with width  $\delta v \ll a_{\text{eff}} \sim \sigma$  (by assumption; see also below).

[3] This region is slowly rotating like a solid body (e.g., due to tidal torques) at a well-defined initial angular frequency  $\Omega$ . In this starting configuration, both dark matter particles and parcels of baryons that are initially located at radius  $r_\infty$  have initial angular momentum  $j = \Omega(r_\infty \sin \theta_0)^2$ , where  $\theta_0$  is the (initial) polar angle in spherical coordinates.

[4] The central region of the collapse flow successfully produces a “seed” black hole in the earliest phases of evolution. The mass of this starting black hole may be much smaller than the large ( $M_{\text{bh}} \sim 10^8 M_\odot$ ) black holes of the final states. Once a black hole has condensed out of the galactic center, it will grow according to the calculations of this model. The initial seed black hole could form by the collapse of the densest (central) part of the perturbation or could be primordial.

The initial state is characterized by two physical variables:  $a_{\text{eff}}$  and  $\Omega$ . We stress that these quantities are not free adjustable parameters, but rather can be specified – or at least constrained – by observations. First, we note that the initial transport speed  $a_{\text{eff}}$  is directly related to (but not equal to) the final velocity dispersion of the final system. In collapsing regions with no dissipation, the virial theorem implies that the scale length of the mass distribution drops by a factor of 2 from the point of maximum expansion (see Binney & Tremaine 1987). Observational considerations (e.g., the “flat rotation curve conspiracy”) suggest that dissipation does not greatly alter the final value of the dispersion  $\sigma$ . This argument implies that the observed velocity dispersion  $\sigma$  is related to the initial transport speed  $a_{\text{eff}}$  of the protogalactic material through the relation  $\sigma^2 = 2a_{\text{eff}}^2$ .

Throughout this paper, we adopt a fiducial value for the starting rotation rate  $\Omega = 6 \times 10^{-2} \text{Myr}^{-1} = 2 \times 10^{-15} \text{ rad s}^{-1}$ , which ultimately provides the observed normalization for the  $M_{\text{bh}} - \sigma$  relation. The scatter about this fiducial value will produce a corresponding scatter in the theoretical  $M_{\text{bh}} - \sigma$  correlation. Although the initial rotation rates of the inner portions of galaxies in their pre-collapse states are no longer observable, this adopted value is in reasonable agreement with expectations. For a ballpark estimate, we can consider the fundamental plane (Binney & Merrifield 1998), which provides a relationship between the half-light radii of galactic bulges and the corresponding velocity dispersions. For a typical value of the velocity dispersion  $\sigma = 200 \text{ km s}^{-1}$ , the effective radius  $R_E$  of a galaxy on the fundamental plane is about 3.5 kpc. In order of magnitude, we expect that  $\Omega \sim \sigma/R_E \sim 2 \times 10^{-15} \text{ rad/s}$ . Rotation rates of this

order of magnitude are also consistent with those expected from observed rotational velocities in galactic bulges (see, e.g., Figure 4.6 of Binney & Tremaine 1987; Binney & Merrifield 1998; Jarvis & Freeman 1985; Wyse & Gilmore 1992).

It is useful to compare our assumptions to the typical value of the spin parameter  $\lambda$  for protogalaxies predicted by numerical simulations (where the angular momentum originates from cosmological torques – see Peebles 1993). Following Bullock et al. (2001), we write the spin parameter in the (slightly non-standard) form

$$\lambda = \frac{J/M}{\sqrt{2}RV_{cir}}, \quad (3)$$

where  $J/M$  is the specific angular momentum,  $R$  is the outer radius, and  $V_{cir}$  is the circular speed of the protobulge structure. For our assumed initial density distribution [2] with solid body rotation, the specific angular momentum  $j = J/M = (2/9)\Omega R^2$  and the circular speed at  $R$  is given by  $V_{cir} = \sqrt{2}a_{\text{eff}}$ . Using these results in the definition [3], we find that  $\lambda = 1/9$  for our assumed initial condition. For comparison, the values of  $\lambda$  that are predicted for dark matter halos by numerical studies of structure formation have a mean value  $\lambda = 0.04-0.05$  (Peebles 1993; Barnes & Efstathiou 1987; Bullock et al. 2001). Although these values are a factor of 2 smaller than used here, they are evaluated for halo mass scales that are thousands of times larger than the protobulge mass scales used here. Notice also that if the bulge forms via collapse with dissipation, then the bulge spin parameter can be larger than the halo spin parameter (e.g., see White 1996).

We can think of the initial conditions  $(a_{\text{eff}}, \Omega)$  in two different ways: First, we can consider the effective transport speed  $a_{\text{eff}}$  and the rotation rate  $\Omega$  as adjustable parameters that can be varied in order to explain four quantities: the velocity dispersion  $\sigma$ , the bulge size scale  $R$ , the bulge mass scale  $M_B$ , and the central black hole mass  $M_{\text{bh}}$ . On the other hand, we can use  $\sigma$  and  $R$  to specify the initial parameters  $a_{\text{eff}}$  and  $\Omega$ . In this latter case, we are left with a theory containing no adjustable parameters, but the theory must still correctly account for the bulge mass scale  $M_B$  and the black hole mass  $M_{\text{bh}}$  as a function of  $\sigma$ .

As we show below, all material with initial conditions given by equation [2] follows a ballistic trajectory as it falls toward the central black hole. This result holds for gas, stars, and dark matter. Gas naturally takes on a centrally concentrated distribution and approaches the form of equation [2]; the gas density obtains this form for the limiting case of hydrostatic equilibrium with an isothermal equation of state. However, the dark matter is somewhat less likely to assume this same starting state. Unlike gas particles, individual dark matter particles can have high angular momentum even if they are part of a larger structure with low (or zero) angular momentum. In other words, it is possible for the dark matter to display the overall density distribution of equation [2], and for the structure as a whole to rotate slowly, and still have the individual particles possess too much angular momentum to be captured. In order for dark matter to fall into the central black hole, the particles must be extremely cold (with internal velocity dispersion  $\delta v \ll a_{\text{eff}} \sim \sigma$ ), and the large scale streaming velocities  $V_S$  in nonradial directions must also be small ( $V_S \ll a_{\text{eff}} \sim \sigma$ ).

Observations have shown that the central black holes of galaxies are strongly correlated with the properties of galactic bulges, but are more weakly correlated with other galactic components such as the disk or the dark matter halo. For example, the galaxy M33 has no bulge (but has both a disk and a dark matter halo), but does not contain a black hole. Although galactic bulges may contain some dark matter, they are probably not dominated by dark matter (e.g., Gerhard et al. 2001). The micro-lensing optical depth of our own Milky Way bulge is high,  $\sim 2 \times 10^{-6}$ , indicating that it contains many baryons in the form of stars, stellar remnants, and brown dwarfs (e.g., Evans & Belokurov 2002). In fact, the baryonic content of our bulge is so high that it is difficult to construct dynamical bulge models using all of the baryons; very little of the mass budget is left over for a significant dark matter component. Dark matter may not play a dominant role in our galactic bulge, and, by extension, may not dominate the determination of the observed  $M_{\text{bh}} - \sigma$  relation.

## 2.2. Classical Orbit Solutions

As the collapse proceeds, particles in the initial distribution fall towards the galactic center. Because the dynamical time scales monotonically increase with radius, infalling shells of material do not cross. The mass contained inside a given spherical shell, which marks a particle’s location, does not change as the particle falls inward and hence orbital energy is conserved. In the classical (nonrelativistic) regime, the orbital energy is given by

$$E = \frac{1}{2}v_r^2 + \frac{1}{2}\frac{j^2}{r^2} - \frac{GM}{r}. \quad (4)$$

In this problem, we consider orbits that begin their collapse trajectories at large radii and then fall a long way toward the center of the galaxy. As a result, we can idealize these trajectories as zero energy orbits.

For a given gravitational potential, we find the orbital solutions for material falling towards the galactic center; the same orbits apply to stars, dark matter, and parcels of gas. In our initial calculation (Paper I), the inner solution is derived using the gravitational potential of a point source. This form is only used in the innermost regime of the collapse flow where the potential is dominated by the forming black hole. In other words, this orbital solution derived here is valid over the range of length scales

$$R_S \ll r \ll r_\infty, \quad (5)$$

where  $R_S$  is the Schwarzschild radius of the black hole and is given by

$$R_S = \frac{2GM}{c^2}. \quad (6)$$

In general, the black hole produced through this collapse process will be rotating so that its event horizon is not completely specified by the Schwarzschild radius  $R_S$ . Notice that at late times, long after black hole formation is complete, dark matter and stars will miss the black hole and continue

to trace through their orbits back out toward large radii; this behavior leads to an extended mass distribution and the potential is no longer well described by a point potential. At these later times of evolution, our solution loses its validity. In the present context, however, we only use the solution during the early phases in which the gravitational potential of the central region is dominated by the black hole. In addition, we note that relativistic corrections become important as  $r \rightarrow R_S$ .

Since this potential is spherically symmetric, angular momentum is conserved and the motion is confined to a plane described by the coordinates  $(r, \phi)$ ; the radius  $r$  is the same in both the plane and the original spherical coordinates. The angular coordinate  $\phi$  in the plane is related to the angle in spherical coordinates by the relation  $\cos \phi = \cos \theta / \cos \theta_0$ , where  $\theta_0$  is the angle of the asymptotically radial streamline (see below). For zero energy orbits, the equations of motion imply a cubic orbit solution,

$$1 - \frac{\mu}{\mu_0} = (1 - \mu_0^2) \frac{j_\infty^2}{GMr} \equiv \zeta(1 - \mu_0^2), \quad (7)$$

where  $j_\infty$  is the specific angular momentum of particles currently arriving at the galactic center along the equatorial plane. The second equality serves to define the parameter  $\zeta$ . Here, the trajectory that is currently passing through the position  $(r, \mu \equiv \cos \theta)$  initially made the angle  $\theta_0$  with respect to the rotation axis (where  $\mu_0 = \cos \theta_0$ ).

For a given angular momentum, we can use equation [4] to determine the pericenter  $p$ , which marks the distance of closest approach for a parabolic (zero energy) orbit. Our assumption of uniform initial rotation implies that  $j_\infty = \Omega r_\infty^2 \sin^2 \theta_0$ , where  $r_\infty$  is the starting radius of the material that is arriving at the center at a given time. The pericenter can be written in the form

$$p = \frac{j^2}{2GM} = \frac{(r_\infty \sin \theta_0)^4 \Omega^2}{2GM} = \frac{(GM)^3 \Omega^2 \sin^4 \theta_0}{2^5 a_{\text{eff}}^8}. \quad (8)$$

In the final equality, we have used  $M = M(r)$  as a label for  $r_\infty$  by inverting the mass distribution of the initial state (equation [2]) to find  $r_\infty = GM/2a_{\text{eff}}^2$ . As in star formation theory (Shu et al. 1987; Cassen and Moosman 1981), we define the centrifugal radius  $R_C$  of the flow according to

$$R_C = \frac{\Omega^2 G^3 M^3}{16 a_{\text{eff}}^8}, \quad (9)$$

which represents the radius of a circular orbit with angular momentum  $j_\infty$  for incoming matter falling within the equatorial plane. For motion in the equatorial plane, this radius  $R_C$  is twice as large as the pericenter  $p$  for a parabolic orbit with the same angular momentum.

Given the orbital solution (equation [7]), we can find the velocity fields for the collapse flow,

$$v_r = - \left( \frac{GM}{r} \right)^{1/2} \left\{ 2 - \zeta(1 - \mu_0^2) \right\}^{1/2}, \quad (10)$$

$$v_\theta = \left( \frac{GM}{r} \right)^{1/2} \left\{ \frac{1 - \mu_0^2}{1 - \mu^2} (\mu_0^2 - \mu^2) \zeta \right\}^{1/2}, \quad (11)$$

$$v_\varphi = \left( \frac{GM}{r} \right)^{1/2} (1 - \mu_0^2) (1 - \mu^2)^{-1/2} \zeta^{1/2}. \quad (12)$$

Since  $\zeta$ ,  $\mu$ , and  $\mu_0$  are related through the orbit equation [7], the velocity field is completely determined for any position  $(r, \theta)$ .

The density distribution of the infalling material can be obtained by applying conservation of mass along a streamtube (Terebey, Shu, & Cassen 1984; Chevalier 1983), i.e.,

$$\rho(r, \theta) v_r r^2 \sin \theta d\theta d\varphi = -\frac{\dot{M}}{4\pi} \sin \theta_0 d\theta_0 d\varphi_0, \quad (13)$$

where  $\dot{M}$  is the total rate of mass flow (inward) through a spherical surface (e.g., Shu 1977). Combining the above equations, we can write the density profile of the incoming material in the form

$$\rho(r, \theta) = \frac{\dot{M}}{4\pi |v_r| r^2} \frac{d\mu_0}{d\mu}. \quad (14)$$

The properties of the collapsing structure determine the orbit equation [7], which in turn determines the form of  $d\mu_0/d\mu$ . With the radial velocity given by equation [10], the density field is thus completely specified in analytical form (implicitly).

Notice that we have ignored gas pressure in the collapse solution. Dark matter and stars always exhibit pressure-free (ballistic) behavior and our approximations are automatically justified for these components. Even for gas, however, the collapse flow always approaches a pressure-free form in the inner region. This (somewhat remarkable) characteristic follows from considering the gaseous portion of the collapse flow to be a scaled-up version of the collapse flows that have been studied previously for star formation theories (Shu 1977; Terebey, Shu, & Cassen 1984; see also Adams 2000). In this case, the collapse of the initial state (with density distribution [2]) proceeds from inside-out and gas parcels in the central portion of the flow always approach ballistic trajectories.

### 2.3. The Mass Scale for Galactic Black Holes

With the collapse solution in place, we can estimate the mass of forming black holes. The collapse flow defines a critical mass scale  $M_C$ , which will be roughly comparable to the final black hole mass. In the earliest stages of collapse, incoming material falls to small radii  $r < R_S$ , where  $R_S$  is the Schwarzschild radius of the forming black hole. The mass that determines  $R_S$  is the total mass  $M = \dot{M}t$  that has fallen thus far, i.e., we assume that the black hole mass  $M_{\text{bh}} = M$  in this early evolutionary stage. As the collapse proceeds, incoming material originates from ever larger radii and carries a commensurate increase in specific angular momentum. The centrifugal barrier of the collapse flow thus grows with time.



If the pericenter  $p$  is sufficiently small, ballistic particles will pass inside the horizon of the black hole and be captured; even particles that pass close to the horizon will be captured (Misner, Thorne, & Wheeler 1973; hereafter MTW). As mass accumulates in the black hole, its horizon scale and capture radius grow linearly with mass. The pericenter of particles in ballistic orbits, falling from our assumed mass distribution, increases as  $p \propto r_\infty^3 \sim M^3$  (equation [8]). In the earliest stages of the collapse, all of the falling material is captured by the black hole. Later, this growth mechanism tapers off when the black hole mass reaches a critical point defined by equating the pericenter  $p$  (for  $\theta = \pi/2$  orbits) to the capture radius of the black hole. In Schwarzschild geometry, particles coming inwards from infinity on zero energy orbits are captured by the black hole if  $p < 4R_S$  (MTW), where  $R_S$  is the Schwarzschild radius (equation [6]). The condition  $p = 4R_S$  defines the critical mass scale  $M_C$ ,

$$M_C \equiv \frac{16a_{\text{eff}}^4}{Gc\Omega} = \frac{4\sigma^4}{Gc\Omega}, \quad (15)$$

which represents the mass at which direct accretion onto the black hole becomes compromised. In the original version of our model (Paper I), this critical mass scale  $M_C$  determined the observed black hole mass  $M_{\text{bh}}$ . Notice that equation [15] displays the correct (observed) scaling with velocity dispersion  $\sigma$ .

Even after the centrifugal barrier grows larger than the Schwarzschild radius, however, the black hole can gain additional mass from material falling on streamlines that are oriented along the rotational poles of the system. After the critical point (described above) is reached, the fraction of the infalling material that lands at such small radii is a relatively rapidly decreasing function of time. As a result, this effect makes the black hole mass larger by a modest factor  $\mathcal{F}_A$ , where the maximum value  $\mathcal{F}_A \approx 1.35$ , as we calculate next:

The mass infall rate  $\dot{M}_{\text{bh}}$  for material falling directly onto the black hole itself is given by

$$\dot{M}_{\text{bh}} = \int_0^1 d\mu 4\pi(\alpha R_S)^2 |v_r| \rho(\alpha R_S, \mu), \quad (16)$$

where  $\mu = \cos \theta$ . We evaluate the density at the capture surface given by  $\alpha R_S$ , where  $\alpha = 8$ . The fact that the capture radius is larger than the Schwarzschild radius is due to the curvature of space by the black hole and is a standard relativistic effect (see MTW). Using equation [14] to specify the density, we can evaluate the integral to obtain a differential equation for the time evolution of the black hole mass, i.e.,

$$\frac{dM_{\text{bh}}}{dt} = \dot{M}_{\text{bh}} = \dot{M}(1 - \mu_C), \quad (17)$$

where  $\mu_C$  is the cosine of the angle of the last streamline (measured from the rotational pole) that falls directly onto the central black hole. Using the orbit equation [7], we find

$$\mu_C = (1 - \alpha R_S/R_C)^{1/2}, \quad (18)$$

where we have evaluated  $\mu_C$  at the black hole surface (keep in mind that  $\mu_C = 0$  for  $R_C < R_S$ ). Next we define dimensionless variables

$$f \equiv M_{\text{bh}}/M_C \quad \text{and} \quad \xi \equiv M/M_C. \quad (19)$$

The reduced black hole mass  $f$  obeys the ordinary differential equation

$$\frac{df}{d\xi} = 1 - (1 - f/\xi^3)^{1/2}. \quad (20)$$

Equation [20] must be integrated subject to the boundary condition  $f = 1$  at  $\xi = 1$  (which means physically that the black hole mass  $M_{\text{bh}} = M_C$  when the centrifugal barrier  $R_C$  first exceeds the Schwarzschild radius  $R_S$ , which is true by definition). If no additional physical effects prevent continued accretion onto the black hole, the enhancement factor is determined by numerically integrating equation [20] to find the limiting value as  $\xi \rightarrow \infty$ . In this limit, the black hole mass grows by an additional factor  $\mathcal{F}_A$  as infall continues along the rotational poles of the system, where

$$\mathcal{F}_A \equiv \lim_{\xi \rightarrow \infty} f(\xi) \approx 1.3502. \quad (21)$$

In other words, the final black hole mass  $M_{\text{bh}} \approx \mathcal{F}_A M_C$ , with  $\mathcal{F}_A \approx 1.35$ , in the absence of additional physical effects.

However, two additional processes can affect this prediction. First, the infalling material can experience shell crossings and the baryonic material can be heated to the system’s virial temperature. As a result, a hot corona forms around the black hole and the infalling material must cross this corona in order to become part of this black hole (anonymous referee; private communication). This effect acts to reduce the effective value of  $\mathcal{F}_A$  and hence equation [21] provides an upper limit. In other words, the enhancement factor  $\mathcal{F}_A$  is confined to the range  $1 < \mathcal{F}_A < 1.35$ . Second, additional material can be added to the black hole through disk accretion; this process is addressed in §3.1.

We can now evaluate the mass scale for forming black holes using our fiducial value of the initial rotation rate  $\Omega$  (see §2.1), equation [15] to set the critical mass scale, and equation [21] to specify the enhancement factor  $\mathcal{F}_A$ . We thereby find the  $M_{\text{bh}} - \sigma$  relation in the form

$$M_{\text{bh}} = \mathcal{F}_A \frac{4\sigma^4}{Gc\Omega} \approx 10^8 M_{\odot} (\sigma/200 \text{ km s}^{-1})^4, \quad (22)$$

where we have written the result in terms of  $\sigma$  rather than  $a_{\text{eff}}$ . This relation is in reasonably good agreement with the observed correlations (see equation [1], Figure 1, and Paper I).

Scatter in the value of the initial rotation rate  $\Omega$  will produce corresponding scatter in the resulting  $M_{\text{bh}} - \sigma$  relation. To obtain an estimate of this effect, suppose that the distribution of  $\Omega$  has the same form as the distribution of the spin parameter  $\lambda$  for galactic halos, where numerical simulations suggest that  $P(\lambda) \propto \exp[-(\ln \lambda/\lambda_0)^2/2\sigma_\lambda^2]$ , with  $\sigma_\lambda \approx 0.5$  (Bullock et al. 2001). If the initial rotation rate  $\Omega$  in this model has the same variance, then the  $M_{\text{bh}} - \sigma$  relation will develop scatter at the level of  $\sigma_\lambda/\ln 10 = 0.22$  dex. This level of scatter is represented in Figure 1 by the bold-faced error bar symbols on the theoretical curve. For completeness, we note that variations in the enhancement factor  $\mathcal{F}_A$  will introduce additional scatter into the  $M_{\text{bh}} - \sigma$  relation. If the parameter  $\mathcal{F}_A$  is uniformly distributed over the range  $1 \leq \mathcal{F}_A \leq 1.35$ , the resulting scatter will

be about 0.04 dex. Since the combined variances of  $\Omega$  and  $\mathcal{F}_A$  add in quadrature (e.g., Richtmyer 1978), the resulting scatter is approximately 0.224 dex (safely smaller than the observed scatter of 0.30 dex).

Most of the baryonic material not captured by the black hole during this early collapse phase eventually forms stars in the galactic bulge. Dark matter with low angular momentum is captured into the black hole along with the baryons; dark matter with high angular momentum ( $p > 4R_S$ ) passes right through the galactic plane and forms an extended structure.

#### 2.4. Bulge Mass Scale and Mass Ratios

This simple dynamical model also predicts a mass scale  $M_B$  for the bulge itself: In the absence of additional physical processes, the collapse of a structure with initial conditions described by equation [2] will produce a “bulge structure” with a well-defined mass scale. Unfortunately, bulge formation is complicated by a host of additional processes (see, e.g., Kauffmann, White, & Guiderdoni 1993; Cole et al. 1994; Somerville & Primack 1999; and especially Kauffmann & Haehnelt 200). The baryonic gas must cool to form the bulge, and the cooling time can be quite long (much longer than the collapse time scales – see the following subsection). Additional gas can be expelled from the bulge through the action of a galactic wind. The dark matter can undergo violent relaxation and only some fraction of the dark matter will remain within the bulge itself. Finally, a significant fraction of the baryonic material can form the inner portion of the galactic disk, rather than remain in the bulge. In spite of these complications, it is interesting to find the mass scale  $M_B$  defined by the dynamical model alone:

If the initial protobulge structure is rotating at angular velocity  $\Omega$ , then only material within a length scale  $R = a_{\text{eff}}/\Omega$  can collapse to form the bulge. Material at larger radii,  $r > R$ , is already rotationally supported and will not fall inwards. In the absence of the aforementioned additional processes, the length scale  $R$  thus defines an effective outer boundary to the collapsing region that forms the bulge (see Terebey et al. 1984 for a detailed calculation of how the rotating, collapsing inner region can match smoothly onto the static, uncollapsing outer region). The boundary  $R$ , in turn, defines a mass scale for the bulge,  $M_B \sim M(R)$ , i.e.,

$$M_B = \mathcal{F}_B \mathcal{F}_{DM} \frac{2a_{\text{eff}}^3}{G\Omega} \approx 3.3 \times 10^{10} M_\odot \mathcal{F}_{DM} (\sigma/200 \text{ km s}^{-1})^3, \quad (23)$$

where the second approximate equality assumes  $\mathcal{F}_{DM} = 1$  and  $\mathcal{F}_B \approx \pi/2$ . The factor  $\mathcal{F}_B$  takes into account the fact that material along the poles can fall into the bulge even though material in the equatorial plane is rotationally supported. The value  $\mathcal{F}_B = \pi/2$  is determined by integrating the initial density distribution (equation [2]) over the entire cylinder defined by  $\varpi < R = a_{\text{eff}}/\Omega$  (where  $\varpi$  is the cylindrical radius). The fraction  $\mathcal{F}_{DM} \leq 1$  is the fraction of the initial mass that is retained within the bulge structure; for example, not all of the dark matter necessarily remains in the bulge.

The resulting expression (equation [23]) shows that the bulge mass scale exhibits power-law behavior with  $M_B \sim \sigma^3$ . It is interesting to compare this result to the observed bulge masses in the sample of galaxies with central black holes. Figure 2 shows the mass scale of equation [23] along with the observed data; also shown is the best fit power-law, which has slope  $\sim 3.3 \pm 0.1$ . For comparison, the traditional Faber-Jackson relation for elliptical galaxies and bulges has the form  $L \propto \sigma^4$  (Binney & Merrifield 1998; Faber & Jackson 1976). Consistency of equation [23] with the Faber-Jackson law would require that  $L \propto M_B^{4/3}$ . For a constant stellar IMF, this relation, in turn, would imply a star formation efficiency  $\epsilon$  of the form  $\epsilon \sim M_B^{1/3}$ . In other words, in order for the mass scale of equation [23] to describe the masses of observed bulges, the more massive systems would have to be more effective at forming stars.

We are also interested in the ratio of black hole mass to bulge mass. In our simple dynamical model, the bulge mass scale  $M_B$  and the black hole mass  $M_{\text{bh}} \approx M_C$  have the same functional dependence on the rotation rate  $\Omega$ . The resulting ratio  $M_{\text{bh}}/M_B \equiv \mu_B$  is independent of  $\Omega$  and is given by

$$\mu_B \equiv \frac{M_{\text{bh}}}{M_B} = \frac{\sqrt{32}}{\mathcal{F}_B} \frac{\sigma}{c} \approx 0.0024 (\sigma/200 \text{ km s}^{-1}). \quad (24)$$

This mass fraction  $\mu_B$  is roughly comparable to the observed ratio of black hole masses to bulge masses in host galaxies. The first estimates suggested that this mass ratio is nearly constant (e.g., Richstone et al. 1998; Magorrian et al. 1998), although the data show appreciable scatter. Later papers found values of  $\mu_B = 0.0015 - 0.0020$  (e.g., Ho 1999; Kormendy 2000), in reasonable agreement with the typical value suggested by equation [24]. More recent work (Laor 2001) finds that the mass ratio is an increasing function of bulge mass,  $\mu_B \propto M_B^{0.53 \pm 0.14}$ , with  $\mu_B \approx 0.0005$  for the smallest bulges with observed black holes and  $\mu_B \approx 0.005$  for bright ellipticals (cf. McLure & Dunlop 2002); this latter result is somewhat steeper than the prediction of this model, which implies  $\mu_B \propto M_B^{1/3}$ . The law [24] is shown in Figure 3 along with the observational data. An unweighted fit to the data implies a slope of  $\sim 0.9$  (close to the model prediction of 1.0), but the error bars and scatter in the data are too large to make a definitive claim. Notice also that the observed black hole scaling law,  $M_{\text{bh}} \sim \sigma^4$ , and the observed scaling law for bulge masses,  $M_B \sim \sigma^{3.3}$ , imply that  $\mu_B \sim \sigma^{0.7}$ .

## 2.5. Time Scales

With an initial density profile of the form  $\rho \sim r^{-2}$ , a detailed collapse calculation (Shu 1977) indicates that the flow exhibits a well defined mass infall rate  $\dot{M} = m_0 a_{\text{eff}}^3 / G$ , where  $m_0 \approx 0.975$  [notice that this starting state corresponds to an unstable hydrostatic equilibrium]. The infall rate is constant in time and we can measure the time elapsed since the collapse began by the total mass  $M$  that has fallen to the galactic center. At early times, all of the mass falling to the center is incorporated into the central black hole. At later times, the mass supply is abruptly shut off by conservation of angular momentum. In this setting, the mass infall rate is quite large,  $\dot{M} \approx 650$

$M_{\odot} \text{ yr}^{-1}$  (for  $\sigma = 200 \text{ km s}^{-1}$  and  $\sigma^2 = 2a_{\text{eff}}^2$ ). The time scale  $\tau_{\text{bh}}$  to form a typical supermassive black hole (with mass  $M_{\text{bh}} \sim 10^8 M_{\odot}$ ) is about  $\tau_{\text{bh}} \sim 10^5 \text{ yr}$ , comparable to the time scale  $\tau_*$  for individual stars to form (e.g., Adams & Fatuzzo 1996; Myers & Fuller 1993). In the absence of any competing physical processes, the dynamical time scale to form the entire bulge is much longer, about  $\tau_{\text{blg}} \sim 25 - 50 \text{ Myr}$ , comparable to the crossing time  $t_{\text{cross}} = R/a_{\text{eff}}$  of the initial structure. One should keep in mind that bulge formation also requires the gas to cool, however, and the cooling time scale can be longer than this dynamical time scale.

### 3. GENERALIZATIONS OF THE MODEL

In this section we present further generalizations of this collapse model for black hole formation. The previous section shows how the black hole gains mass through infall from the collapse flow. However, additional mass can be added to the black hole through disk accretion (§3.1). Furthermore, black holes formed through this collapse picture are born rapidly rotating (§3.2). The scaling relation for the black hole mass  $M_{\text{bh}}$  as a function of  $\sigma$  depends on the initial angular momentum profile of the pre-collapse material; in fact, the angular momentum distribution is the most important determining factor in specifying the black hole masses (see §3.3, 3.4). This model can also be generalized include the effects of mergers (§3.5) and non-spherical initial conditions (in particular, quadrupole moments; see §3.6).

#### 3.1. Disk Accretion

Material that falls to the midplane of the system in gaseous form can collect into a disk structure that surrounds the nascent black hole. The presence of the disk is consistent with the current theoretical ideas about active galactic nuclei and the jets they produce. In order to retain the desired scaling law  $M_{\text{bh}} \sim \sigma^4$ , however, the total amount of mass added to the black hole through disk accretion should be less than (or at most comparable to) the original mass scale  $M_C$ .

The energy density of the universe from quasar activity places a limit on the amount of mass that can be accreted by black holes. This energy density  $U_T$  has been estimated to be  $U_T \approx 2.5 \times 10^{-15} \text{ erg/cm}^3$  (Elvis, Risaliti, & Zamorani 2002). If this energy arises from mass accretion onto black holes with energy conversion efficiency  $\epsilon$ , then the energy density  $U_T$  implies a corresponding minimum mass density in black holes at the present cosmological epoch. Two recent papers (Elvis et al. 2002; Yu & Tremaine 2002) have estimated the amount of mass accreted through quasar activity over the redshift range  $0 \leq z \leq 5$ . The mass density in black holes due to accretion activity takes the form  $\rho_{\text{acc}} \approx 2.1 \times 10^5 [0.1(1 - \epsilon)/\epsilon] M_{\odot} \text{ Mpc}^{-3}$ . For comparison, the observed  $M_{\text{bh}} - \sigma$  relation implies a present day mass density in black holes  $\rho_{\text{bh}} \approx 2.5 \times 10^5 M_{\odot} \text{ Mpc}^{-3}$  (Yu & Tremaine 2002; Aller & Richstone 2002). The present ratio of the accreted mass to the observed mass is thus  $\mathcal{R} = 0.083 (1 - \epsilon)/\epsilon$ . In order for the infall collapse model of this paper

to explain the observed black hole masses, the ratio  $\mathcal{R} < 1$  and hence the conversion efficiency must be at least  $\epsilon \sim 0.08$ . If the efficiency of energy conversion in quasars is too low, then black holes would gain more mass from disk accretion than from infall. If the energy conversion efficiency is high, however, quasar light could be explained by a modest addition of mass, and some other physical process (e.g., infall) would be required to explain the observed black hole masses.

Because of the present observational uncertainties, the critical value of  $\epsilon_C$  (the value required for disk accretion to explain the observed mass density in black holes) is not completely specified. Using only the quasar constraint, Yu & Tremaine (2002) find  $\epsilon_C \approx 0.1$ , whereas Elvis et al. (2002) find  $\epsilon_C \approx 0.15$ . For Schwarzschild black holes, the energy conversion efficiency is expected to be about  $\epsilon \sim 0.1$ , but higher efficiency, with  $\epsilon \sim 0.2$ , is possible for thin-disk accretion onto a Kerr black hole (see Yu & Tremaine 2002). A plausible upper limit for accretion processes is  $\epsilon = 0.31$  (Thorne 1974). Both the observations of background radiation and the theoretical expectations for energy conversion efficiency  $\epsilon$  should be specified further to resolve this issue.

For comparison, we can derive another constraint on the amount of accreted mass. This constraint is more general than in the discussion above, but is also weaker. We consider the limiting case in which disk accretion is maximally effective. Disk accretion generally cannot operate faster than the orbit time at the outer disk edge (Shu 1992). In this context, the orbit time  $\tau$  is given by

$$\tau^2 = \frac{4\pi^2 R_C^3}{GM} = \frac{4\pi^2 \Omega^6 (GM)^8}{\sigma^{24}}. \quad (25)$$

When the disk accretion time becomes longer than the time required for the disk to condense into stars, i.e., when  $\tau > \tau_*$ , disk accretion is no longer effective and the mass flow onto the central black hole must come to an end. This condition implies a maximum mass scale for accreting black holes. The mass appearing in equation [25] above represents the total mass that has fallen to the center by a given time. Only a fraction of this mass is available to join the disk because only a fraction  $f_B$  is baryonic and a fraction  $f_G$  is in gas (rather than in stars). Including these two factors, the maximum mass that can be added to the black hole via disk accretion becomes

$$M_{\max} = (2\pi)^{-1/4} f_B f_G (\sigma^3/G)(\tau_*/\Omega^3)^{1/4}. \quad (26)$$

For typical values of the input parameters  $\sigma$  and  $\Omega$ , and for  $f_B = 2/15$ ,  $f_G = 1/2$ , this maximum mass scale is about 5 times larger than  $M_C$ . In the limit of maximally efficient disk accretion, the mass scale  $M_C$  defined by the centrifugal radius can thus be compromised (see also Burkert & Silk 2001; Silk & Rees 1998). Unfortunately, the disk accretion rates are not known in these early stages of galaxy formation (however, see Kumar 1999). In most known astrophysical disks, the disk accretion rates are much smaller than their maximum values, typically by factors of  $10^2 - 10^4$  (e.g., Shu 1992), which would imply that most of the black hole mass does not come from accretion. On the other hand, as discussed above, the observed X-ray background implies that the central black holes that power quasars must accrete a substantial mass, roughly comparable to the masses obtained via infall. This argument assumes that the mass in the disk is large enough to affect the black hole mass; however, the infall model used here naturally places most of the incoming mass at large radii appropriate for the disk (e.g., Cassen & Moosman 1981).

### 3.2. Black Hole Angular Momentum

This theoretical model for supermassive black hole formation predicts that the resulting black holes should be rotating rather rapidly. If we approximate the orbital solutions for incoming material using the classical treatment of §2.2 and the effective capture radius of a Schwarzschild black hole, then the angular momentum  $J_{\text{bh}}$  of the resulting black hole takes the form

$$J_{\text{bh}} = \frac{1}{9} 2^{11} a_{\text{eff}}^8 c^{-3} G^{-1} \Omega^{-2}. \quad (27)$$

In the absence of additional mass sources, we can write this angular momentum in terms of the black hole mass  $M_{\text{bh}} = M_C$  and the Schwarzschild radius  $R_S$ ,

$$J_{\text{bh}} = \frac{4}{9} c M_{\text{bh}} R_S \approx 0.44 c M_{\text{bh}} R_S. \quad (28)$$

The maximum allowed value for the numerical coefficient in equation [28] is 0.5 (e.g., Thorne, Price, & MacDonaold 1986; Blandford 1990), so these black holes are rotating close to their maximum rates. Notice that relativists usually write the Kerr metric in terms of the parameter  $a \equiv J/M$ . In units where  $G = 1$ , this parameter has a maximum value of  $a = M$ . This theory predicts the formation of black holes with the ratio  $a/M \approx 0.89$  – close to its maximum value of unity. Continued infall will add both mass and angular momentum to the black hole, and will change this prediction somewhat. Notice also that disk accretion models predict that supermassive black holes should be rotating rapidly (e.g., Elvis et al. 2002).

Keep in mind that this result uses mixed approximations. We have derived the maximum mass scale using the capture radius appropriate for Schwarzschild geometry and purely classical orbits solutions. The resulting black holes are rapidly rotating, however, and curve space-time as described by the Kerr metric. A fully self-consistent calculation should find orbit solutions and the capture radius for Kerr black holes, with the angular momentum parameter  $a_J = J_{\text{bh}}/M_{\text{bh}}$  determined at each evolutionary stage by conservation of angular momentum. This calculation is beyond the scope of this present paper, but could change our results at the level of 50 percent.

The last stable orbit for the Kerr metric can be worked out in terms of simple functions (e.g., Riffert 2000); the last stable orbit for Kerr geometry is smaller than that of Schwarzschild geometry, and the last captured streamline should behave similarly. In other words, a Kerr black hole has a smaller surface area than a Schwarzschild black hole of the same mass (e.g., Rees 1984). As the black hole grows, it gains both mass – which makes its capture cross section larger – and angular momentum – which makes its capture cross section smaller. Near the end of the infall phase, the added angular momentum to the black hole decreases its cross section, and the infalling material starts to have too much angular momentum to fall within the older, larger cross section. This effect thus acts to make the transition more abrupt.

### 3.3. General Initial Conditions

The success of this simple model for black hole formation rests on the initial angular momentum profile, which must have a particular form. In order to determine how sensitive the results are to the assumed initial conditions, we consider generalized initial density distributions of the form

$$\rho(r) = Ar^{-\Gamma}, \quad (29)$$

where  $A$  is a constant and  $\Gamma$  is an arbitrary index. As before, we assume that the initial structure is rotating at a uniform rate  $\Omega$ . The corresponding mass distribution is given by

$$M(r) = \frac{4\pi A}{3-\Gamma} r^{3-\Gamma} \equiv \tilde{A} r^{3-\Gamma}, \quad (30)$$

where we have defined a reduced constant  $\tilde{A} \equiv 4\pi A/(3-\Gamma)$ . To find the black hole mass scale resulting from the collapse of this initial state, we use the same criterion as before, which takes the form  $j_\infty = 4GM/c$ , where  $j_\infty = \Omega r_\infty^2$ . To specify the starting radius  $r_\infty$ , we must invert the mass distribution to obtain

$$r_\infty = \left[ \frac{M}{\tilde{A}} \right]^{1/(3-\Gamma)}. \quad (31)$$

Solving for the black hole mass scale, we obtain

$$M_{\text{bh}} = \left[ \frac{4G}{c\Omega} \right]^{(3-\Gamma)/(\Gamma-1)} \tilde{A}^{2/(\Gamma-1)}, \quad (32)$$

where we must restrict the analysis to  $\Gamma > 1$ . For less steep initial density distributions, the centrifugal barrier of the collapse flow increases more slowly with mass than does the capture radius of the black hole (which has a linear dependence).

We can also solve for the other parameters of the forming bulge system. The radius  $R$  that marks the outer boundary is given by

$$R = \left[ \frac{\tilde{A}G}{\Omega^2} \right]^{1/\Gamma}, \quad (33)$$

while the bulge mass scale takes the form

$$M_B = \left[ \frac{G}{\Omega^2} \right]^{3/\Gamma-1} \tilde{A}^{3/\Gamma}. \quad (34)$$

With the radius  $R$  and bulge mass scale defined, we can solve for the expected velocity dispersion of the final system using the relation  $\sigma^2 \approx 2GM_B/R$ , where the factor of 2 arises from the collapse itself. The resulting expression for the velocity dispersion is

$$\sigma = \sqrt{2} \Omega^{1-2/\Gamma} \left[ \tilde{A}G \right]^{1/\Gamma}. \quad (35)$$



With this expression for  $\sigma$  in hand, we can write the expected bulge mass  $M_B$ , bulge size scale  $R$ , and black hole mass  $M_{\text{bh}}$  in terms of  $\sigma$  rather than the initial variable  $A$  (or  $\tilde{A}$ ) appearing in the density distribution, i.e.,

$$M_B = \frac{\sigma^3}{2\sqrt{2}\Omega G}, \quad R = \sigma/(\sqrt{2}\Omega), \quad \text{and} \quad M_{\text{bh}} = \frac{\sigma^4}{cG\Omega} \left[ \sqrt{8}\frac{\sigma}{c} \right]^{(4-2\Gamma)/(\Gamma-1)}. \quad (36)$$

And finally, we obtain the corresponding expression for the mass ratio:

$$\mu_B = \left[ \sqrt{8}\frac{\sigma}{c} \right]^{(3-\Gamma)/(\Gamma-1)}. \quad (37)$$

This result is *very* sensitive to the starting slope  $\Gamma$  of the density profile (for an assumed constant rotation rate  $\Omega$ ). If the index  $\Gamma$  is much smaller (larger) than the preferred value  $\Gamma = 2$ , then the final black hole masses are much smaller (larger) than those observed. Variations in the slope  $\Gamma$  will produce corresponding scatter in the observed  $M_{\text{bh}} - \sigma$  relation; as a benchmark, variations at the level of  $\Gamma = 2 \pm 0.1$ , will produce scatter of about 0.5 dex. The value of the index  $\Gamma$  affects this model for mass scales  $M_S$  in the range  $0.1M_{\text{bh}} < M_S < 0.5M_B$ .

In summary, this model is sensitive to the form of the initial conditions. Moderate departures from our assumed starting condition  $\rho \sim r^{-2}$  to large variations in the predicted black hole masses  $M_{\text{bh}}$  and mass ratios  $\mu_B$ . If this model is correct, then the relevant initial conditions for the collapse of galactic bulges *must* have angular momentum distributions close to those assumed here (specified by equation [2]).

### 3.4. Dimensional Analysis

Given all of the generalized relations discussed in the previous section, how can we make sense of all the possibilities? For this theoretical model, the story is relatively simple: For the formation of the bulge itself, the black hole forming at the galactic center has essentially no effect. Because no relativistic effects come into play, the speed of light  $c$  does not enter into the formulae describing the bulge properties  $\sigma$ ,  $M_B$ , and  $R$ . The only variables that can determine these quantities are the rotation rate  $\Omega$ , the parameters of the initial density distribution ( $A$  and  $\Gamma$ ), and the gravitational constant  $G$ . Furthermore, the index  $\Gamma$  is dimensionless, so the only quantities that carry dimensions are  $A$ ,  $\Omega$ , and  $G$ . A simple virial argument lets us replace the density coefficient  $A$  with the velocity dispersion  $\sigma$ , which is a much more familiar quantity. For a given velocity scale  $\sigma$ , the quantity  $\sigma^3/G$  defines a mass infall rate; when combined with a time scale  $\Omega^{-1}$  (which is the only time scale present in this simple treatment) we thus obtain the mass scale  $M \sim \sigma^3/G\Omega$ , which we identify as the bulge mass scale  $M_B$ . To summarize, the three quantities with dimensions ( $A$ ,  $G$ ,  $\Omega$ ) can only define the three bulge quantities ( $\sigma$ ,  $M_B$ ,  $R$ ) in one way (up to dimensionless factors of order unity).

Next, however, we must put the black hole mass into the problem. The black hole introduces relativistic effects and, in particular, introduces the speed of light  $c$  as another fundamental

constant. The ratio  $\beta = \sigma/c$  is another dimensionless parameter in the problem. In terms of dimensional analysis, we can now define an infinite number of new scales. For example, in addition to the bulge mass scale  $M_B$ , we now have the family of mass scales  $M = F(\beta)M_B$ , where  $F(\beta)$  is an unspecified function of the second dimensionless field  $\beta$ . In our treatment, the power-law forms for the initial conditions lead to new mass scales given by the power-laws  $M_\eta = M_B \beta^\eta$ , where  $\eta$  can be any real number. The physical law of angular momentum conservation, in conjunction with the initial profile, chooses the value of the exponent  $\eta$  for a given model. In the simplest case, that of isothermal  $\rho \sim r^{-2}$  initial conditions, we obtain  $\eta = 1$  and hence  $M_{\text{bh}} \sim M_B(\sigma/c)$ , which happens to be the observed scaling law ( $M_{\text{bh}} \sim \sigma^4$ ). Notice also that the ratio  $M_{\text{bh}}/M_B \sim \sigma/c \sim 10^{-3}$  (the observed order of magnitude). The other (more general) choices of initial conditions,  $\rho \sim r^{-\Gamma}$ , thus correspond to other possible values of the exponent  $\eta$ , i.e.,  $\eta = (3 - \Gamma)/(\Gamma - 1)$ .

### 3.5. Survival of Scaling Laws with Mergers

Many galaxies are expected to experience merger events during their formative stages of evolution (e.g., White & Rees 1978; White 1979). If the initial collapse of protobulges proceeds as envisioned in the simple theoretical model developed in this paper, then the fundamental building blocks of galaxies will have bulge mass  $M_B \sim \sigma^3$  and black hole masses  $M_{\text{bh}} \sim \sigma^4$ . However, observations indicate that the *final* merger products obey these scaling relations. As a result, we must now consider what happens to these scaling laws if the fundamental building blocks undergo multiple merger events (see also Hughes & Blandford 2002; Menou, Haiman, & Narayanan 2001; Ebisuzaki et al. 2001; Volonteri, Haardt, & Madau 2003).

For the sake of this discussion, we consider the rotation rate to be constant so that the only relevant variable is the velocity dispersion  $\sigma$ . We define a dimensionless variable  $s = \sigma/(200 \text{ km s}^{-1})$ . If protobulges merge many times and if they all contain central black holes that merge, then the final black hole mass can be written in the form

$$M_{\text{bhf}} = \sum_j M_{\text{bh}j} = M_0 \sum_j s_j^4, \quad (38)$$

where we assume in the second equality that the starting units, labeled by the index  $j$ , obey the scaling law derived in §2 (and Paper I). All sums are taken up to  $N$ , which specifies the number of protobulges (initial units) that merge to form the final stellar system. Notice that this equation assumes minimal energy losses from gravitational radiation during the collisions.

We must relate the velocity dispersion  $s_f$  of the final bulge system to the velocity dispersions  $s_j$  of the individual units. We first consider one idealized limiting case: If the mergers take place with zero orbital energy and no energy losses occur during the collision, then the final energy of a merged system must equal the internal energies of the initial (pre-merger) pairs. If we consider the systems to be in virial equilibrium and to be homologous (a gross approximation, but a good

place to start for conceptual purposes), we obtain the relation

$$s_f^2 = \sum_j p_j s_j^2, \quad (39)$$

where we have defined  $p_j \equiv R_{Bj}/R_{Bf}$ .

Now let us define  $q_j \equiv s_j^2$  for all protobulges labeled by the index  $j$ . We can think of the  $q_j$  and the  $p_j$  as components of  $N$ -dimensional vectors (which live in the space of protobulge parameters). With this ansatz, we can write the final black hole mass in the form

$$M_{\text{bh}f} = M_0 \sum_j q_j^2 = M_0 |q_j|^2, \quad (40)$$

where the notation  $|q_j|^2$  denotes the vector magnitude squared; the final velocity dispersion  $s_f$  takes the form

$$s_f^2 = \mathbf{p} \cdot \mathbf{q} \quad \Rightarrow \quad s_f^4 = |p_j|^2 |q_j|^2 \cos^2 \theta_{\text{bh}}, \quad (41)$$

where  $\theta_{\text{bh}}$  is the angle between the two vectors in bulge parameter space. Combining the above equations, the final black hole mass takes the suggestive form

$$M_{\text{bh}f} = \frac{M_0 s_f^4}{|p_j|^2 \cos^2 \theta_{\text{bh}}}. \quad (42)$$

The final mass of the black hole thus displays a quartic dependence on the final velocity dispersion (to leading order). Some intrinsic scatter will be introduced through varying angles  $\theta_{\text{bh}}$  and mass weights  $p_j$ . We can consider the limiting case in which all of the starting protobulge units are identical,  $p_j = 1/N$  for all units  $j$ , and the two vectors  $p_j$  and  $q_j$  are parallel so that  $\cos \theta_{\text{bh}} = 1$ . In this limit, the final black hole mass takes the form  $M_{\text{bh}} = N M_0 s_f^4$ , which is consistent with the observed scaling relation (equation [1]). In other words, the scaling law can be preserved under the action of mergers in this idealized limit.

We can also find the behavior of the bulge mass under repeated merger events. The final bulge mass  $M_{Bf}$  after  $N$  mergers is given by

$$M_{Bf} = M_{B0} \sum_j s_j^3 = M_{B0} \sum_j s_j q_j = M_{B0} \mathbf{s} \cdot \mathbf{q}. \quad (43)$$

We can write the dot product in terms of another angle  $\theta_B$ ,

$$\mathbf{s} \cdot \mathbf{q} = |s_j| |q_j| \cos \theta_B, \quad (44)$$

which allows us to write the final bulge mass in the form

$$M_{Bf} = M_{B0} |s_j| s_f^2 \left\{ \frac{\cos \theta_B}{|p_j| \cos \theta_{\text{bh}}} \right\}. \quad (45)$$

To explicitly illustrate the possibility of preserving the  $M_{\text{bh}} - \sigma$  relation under the action of mergers, we have performed a simple set of Monte Carlo simulations, as depicted in Figure 4. In these numerical experiments, the number of interacting units is randomly chosen within the range  $2 \leq N \leq 6$  (see, e.g., Wechsler et al. 2002). The velocity dispersions of the interacting units are chosen to be random, but logarithmically spaced in order to evenly sample the observed range of (final)  $\sigma$ . The radial sizes of the interacting units  $p_j = R_{jB}/R_{fB}$  are chosen to be equal so that  $p_j = 1/N$ . In order to get the normalization correct, we let the mass scale  $M_0$  of the interacting units (equation [38]) be a factor of three smaller than that of the observationally determined distribution (equation [1]). Notice that this approximation is equivalent to allowing serious energy losses during the merger events. The final values of the black hole mass and velocity dispersion are then calculated according to equations [38] and [39]. With these idealizations, the final distribution retains its power-law form and appears to be in good agreement with the observed correlation (see Figure 4). We stress, however, that the range of parameter space available for merging protobulges is enormous – not every merger scenario will produce such a clean correlation. We leave a more detailed exploration of parameter space for future work.

### 3.6. The Effects of Initial Quadrupole Moments

In this subsection, we consider the effects of a quadrupole moment on this collapse picture of black hole formation. Since the protobulge structures can obtain their initial rotation rates through tidal torques acting on nonzero quadrupole moments of the mass distribution, it is important to check whether such quadrupole moments affect the collapse flow. We can consider two limiting cases: A substantial quadrupole moment in the inner regime and a substantial quadrupole on the large size scale of the protobulge itself. The case of the inner regime is very much like the binary star potential in the star formation problem, and this situation has already been shown to have little effect (Allen 1999, Jijina 1999). We thus consider the case of an outside quadrupole moment.

As a starting point, we consider the outer quadrupole to be akin to two point masses  $M$  with separation  $R$ . In order for the outer quadrupole to exert a torque on the inner region (the portion of the pre-collapse structure that will eventually comprise the black hole), the inner region must also have a quadrupole moment. We consider the inner portion to have a dumbbell shape with mass scale  $m$  and size  $\ell$ . The force exerted on the inner region by the outer quadrupole is given by the tidal force law

$$F \approx \frac{GMm}{R^2} \frac{\ell}{R}. \quad (46)$$

The torque  $\tau$  exerted on the inner region is given by this force acting through a lever arm of size  $\ell$ . The torque is given by

$$\tau \approx \frac{GMm\ell^2}{R^3}. \quad (47)$$

Now we need to make the connection between these quantities and the scales in the black hole formation problem. The size scale  $R$  is the size of the protobulge, i.e.,  $R \approx a_{\text{eff}}/\Omega$ . Because the

mass distribution has the profile of an isothermal sphere ( $\rho \sim r^{-2}$  and  $M(r) \sim r$ ), the size  $\ell$  is smaller than  $R$  by the ratio of the black hole mass to the bulge mass, i.e.,  $\ell/R = \mu_B$ . The mass  $M$  of the outer quadrupole is given by  $M = \lambda_1 M_B$ , where the dimensionless parameter  $\lambda_1$  determines the asphericity of the configuration. If the distribution is perfectly spherical,  $\lambda_1 \rightarrow 0$ . In the limit that the protobulge has a dumbbell shape,  $\lambda_1 \rightarrow 1$ . Similarly, we let  $m = \lambda_2 M_{\text{bh}}$ . With these definitions, the torque can be written in terms of the physical quantities in our paper as

$$\tau = \lambda_1 \lambda_2 \mu_B^2 \frac{GM_B M_{\text{bh}}}{R}. \quad (48)$$

One way to quantify the effect of this torque on the collapse flow is to find the total change in angular momentum produced by the torque, which acts over the collapse time  $\Delta t$  of the inner region only. (After the black hole has formed, the still-existing outer quadrupole will not effect the black hole mass). The time for the inner region to collapse is given by

$$\Delta t \approx M_{\text{bh}}/\dot{M} = \frac{GM_{\text{bh}}}{a_{\text{eff}}^3} = \frac{2M_{\text{bh}}}{M_B \Omega} = \frac{2\mu_B}{\Omega}. \quad (49)$$

Combining the above expressions for the torque and the time interval over which it acts, we find the change in angular momentum:

$$\Delta J = 2\lambda_1 \lambda_2 \mu_B^2 \frac{GM_{\text{bh}}^2}{R\Omega}. \quad (50)$$

For later convenience, we note that our model implies  $GM_B/R^3 = 2\Omega^2$ , so we rewrite the above expression to obtain the form

$$\Delta J = 4\lambda_1 \lambda_2 \mu_B M_{\text{bh}} \Omega \ell^2. \quad (51)$$

The starting angular momentum  $J_0$  of the inner region can be obtained by integrating over the initial density distribution. The result is

$$J_0 = \frac{2}{9} M_{\text{bh}} \Omega \ell^2. \quad (52)$$

The resulting fractional change in the angular momentum of the inner region is immediately found to be

$$\frac{\Delta J}{J_0} = 18\lambda_1 \lambda_2 \mu_B. \quad (53)$$

The mass fraction  $\mu_B \approx 0.0024$  in our model, so this fraction change becomes

$$\frac{\Delta J}{J_0} \approx 0.043\lambda_1 \lambda_2. \quad (54)$$

Even in the extreme limit of highly developed quadrupole moments on both the inside and the outside, the fractional change in angular momentum is only about 4 percent. In a more realistic case, the outer quadrupole should be smaller than unity  $\lambda_1 < 1$ , but still large enough to give the bulge an elliptical appearance; the inner region can be smoothed out (e.g., see Peebles 1993 for streaming arguments) and the inner quadrupole should also have  $\lambda_2 < 1$ . In any case, the coupling between the outer quadrupole moment and the inner collapse region can be considered weak in the context of our orbit solutions.

## 4. CONCLUSIONS

In this contribution, we have presented further development of the simple theoretical model for supermassive black hole formation that was put forth in Paper I. This model begins with an initial state specified by a density distribution of the form  $\rho = a_{\text{eff}}^2/2\pi Gr^2$  and a uniform rotation rate  $\Omega$ . The parameters  $(a_{\text{eff}}, \Omega)$  represent the specification of the initial conditions. As the initial state collapses to form a galactic bulge, the collapse flow produces a black hole in the center. The velocity dispersion of the final bulge system is comparable to the effective transport speed and we make the identification  $\sigma \approx \sqrt{2}a_{\text{eff}}$ . In developing this basic picture, we find the following results:

[1] The black hole mass  $M_{\text{bh}}$  is determined by the condition that the centrifugal radius exceeds the capture radius of the central black hole. This requirement leads to the scaling law  $M_{\text{bh}} = M_0(\sigma/200 \text{ km s}^{-1})^4$ , which is consistent with observations both in its dependence on velocity dispersion  $\sigma$  and for the mass scale ( $M_0 \approx 10^8 M_\odot$ ) of the leading coefficient (see equation [22] and Figure 1). The mass scale  $M_0$  is given by  $M_0 = 4\mathcal{F}_A(200\text{km/s})^4/cG\Omega$ , so that variations in the rotation rate  $\Omega$  and the amount of continued infall  $\mathcal{F}_A$  lead to dispersion about the observed power-law correlation. If the initial rotation rate  $\Omega$  follows the same distribution as that calculated for the spin parameter  $\lambda$  of dark matter halos, then variations in  $\Omega$  would produce a scatter of  $\sim 0.22$  dex (a factor of  $\sim 1.7$ ) in the predicted  $M_{\text{bh}} - \sigma$  scaling law. The observed relation has a factor of 2 dispersion.

[2] A bulge mass scale is defined in this model by the outer boundary of the collapsing region. Material at initial radii  $r > R$  is rotationally supported and cannot collapse, where  $R = a_{\text{eff}}/\Omega$ . This condition implies a scaling law for the bulge mass scale,  $M_B = 2\mathcal{F}_B a_{\text{eff}}^3/G\Omega \propto \sigma^3$  (see equation [23] and Figure 2). Although bulge formation must involve physical processes that are not included in this dynamical model (e.g., gas cooling, feedback from galactic winds, disk formation), this scaling law for  $M_B$  is nonetheless in good agreement with the observed relation for host galaxies that contain supermassive black holes, as shown in Figure 2.

[3] If we interpret the bulge mass scale  $M_B$  (see [2] above) as the bulge mass itself, then this model predicts the ratio  $\mu_B$  of black hole mass to bulge mass (equation [24] and Figure 3). The theoretical mass ratio is proportional to the velocity dispersion and has the form  $\mu_B \approx 0.0024(\sigma/200 \text{ km s}^{-1})$ , roughly comparable to observed mass ratios. A mass ratio  $\mu_B$  that increases with velocity dispersion  $\sigma$  is consistent with (and even indicated by) a recent analysis of the observational data (Laor 2001); an unweighted least squares fit to the data shown in Figure 3 implies a slope of  $\sim 0.9$ . We also note that a constant mass ratio  $\mu_B$  may be inconsistent with the data: Since the black hole mass scales as  $M_{\text{bh}} \sim \sigma^4$  (Tremaine et al. 2002), a constant mass ratio  $\mu_B$  would require the bulge mass to also scale as  $M_B \sim \sigma^4$ . However, the observed bulge masses (for systems with detected black holes) do not indicate such a steep dependence on  $\sigma$ ; the data suggest an index of approximately  $3.3 \pm 0.1$  (see Figure 2).

[4] In this scenario, the black hole forms quickly, with a typical formation time of  $\sim 10^5$  yr.

[5] The black holes formed through this mechanism are born with rapid rotation rates. As a result, the geometry in the central regions is best described by the Kerr metric. Specifically, this model predicts that supermassive black holes are formed with an initial rotation parameter  $a/M \approx 0.9$ , relatively close to the maximum value of  $a/M = 1$ . Such high black hole rotation rates may be detectable by LISA (the Laser Interferometer Space Antenna).

[6] Although the supermassive black holes produced by this process are intrinsically relativistic objects, relativistic effects play only a modest role in the collapse flows that produce them. The most important effect is that the capture radius of a black hole is larger than the Schwarzschild radius by a factor of 4 and this effect leads to black hole masses that are larger by this same factor.

[7] The predicted black hole masses are very sensitive to the initial conditions. For an initial density distribution of the form  $\rho \sim r^{-2}$  (with constant angular velocity  $\Omega$ ), the subsequent collapse produces black holes and galactic bulges with the correct masses and the correct dependence on velocity dispersion  $\sigma$ . The correct mass normalization depends on the choice of rotation rate  $\Omega \approx 2 \times 10^{-15}$  rad/s. Initial density profiles with shallower slopes,  $\rho \sim r^{-\Gamma}$  with  $\Gamma < 2$ , produce *smaller* black holes with a *steeper* slope in the  $\log M_{\text{bh}} - \log \sigma$  plane. In general, the initial profile of specific angular momentum – given by the combination of  $\rho(r)$  and  $\Omega(r)$  – determines the final mass scales. This sensitivity on initial conditions is both the strongest and weakest aspect of the model: If we can unambiguously determine the angular momentum distribution of the initial states, we can directly verify or falsify this theoretical scenario for black hole and bulge formation. We also note that our initial conditions apply on (initial) radial scales of several kpc. The manner in which these initial conditions match onto the Hubble flow and the larger scale structure of the galactic halo (at radial scales of many hundred kpc) remain to be determined.

[8] If galactic bulges and larger galactic structures are formed through the mergers of smaller constituent pieces, this scenario for black hole formation can still play a role: In this case, a number of the constituent pieces would form black holes in their centers through this mechanism. The resulting scaling laws (e.g.,  $M_{\text{bh}} \sim \sigma^4$ ) can be preserved, or nearly preserved, under mergers for idealized circumstances (§3.5). On the other hand, mergers tend to reduce the angular momentum per unit mass, so that merger scenarios predict a lower angular momentum for the resulting black holes (e.g., Hughes & Blandford 2002). Future measurements of the angular momentum of supermassive black holes are thus crucial for discriminating between various formation scenarios.

We would like to thank Gus Evrard, Karl Gebhardt, and Risa Wechsler for useful discussions; we especially thank Rosie Wyse for enlightening discussions regarding bulge rotation rates. Finally, we thank an anonymous referee for many suggestions that improved the paper. This work was supported by NASA through the Long Term Space Astrophysics program and the Space Telescope Science Institute, and by the University of Michigan through the Michigan Center for Theoretical Physics.

## REFERENCES

- Adams, F. C. 2000, *ApJ*, 542, 964, astro-ph/0006231
- Adams, F. C., & Fatuzzo, M. 1996, *ApJ*, 464, 256
- Adams, F. C., Graff, D. S., & Richstone, D. O. 2001, *ApJ*, 551, L31, astro-ph/0010549 (Paper I)
- Allen, A. 1999, PhD Thesis, Univ. California, Berkeley
- Aller, M. C., & Richstone, D. 2002, *AJ*, 124, 3035
- Barnes, J., & Efstathiou, G. 1987, *ApJ*, 319, 575
- Binney, J., & Merrifield, M. 1998, *Galactic Astronomy* (Princeton: Princeton Univ. Press)
- Binney, J., & Tremaine, S. 1987, *Galactic Dynamics* (Princeton: Princeton Univ. Press)
- Blandford, R. D. 1990, in *Active Galactic Nuclei*, ed. R. D. Blandford, H. Netzer, & L. Woltjer (Springer)
- Blandford, R. D. 1999, in *Origin and Evolution of Massive Black Holes in Galactic Nuclei*, ed. D. Merritt, M. Valluri & J. Sellwood, (San Francisco: ASP), p. 87, astro-ph/9906025
- Bullock, J. S., Dekel, A., Kolatt, T. S., Kravtsov, A. V., Klypin, A. A., Porciani, C., & Primack, P. R. 2001, *ApJ*, 554, 85
- Burkert, A., & Silk, J. 2001, *ApJ*, 554, 151
- Carollo, C. M., Stiavelli, M. & Mack, J. 1998, *AJ*, 116, 68
- Cassen, P., & Moosman, A. 1981, *Icarus*, 48, 353
- Chevalier, R. 1983, *ApJ*, 268, 753
- Ciotti, L., & Ostriker, J. P. 1997, *ApJ*, 487, L105
- Ciotti, L., & Ostriker, J. P. 2001, *ApJ*, 551, 131
- Cole, S., et al. 1994, *MNRAS*, 271, 781
- Daniel, J., & Loeb, A. 1995, *ApJ*, 443, 11
- Ebisuzaki, T. et al. 2001, *ApJ*, 562, L19
- Elvis, M., Risaliti, G., & Zamorani, G. 2002, *ApJ*, 565, L75, astro-ph/0112413
- Evans, N. W., & Belokurov, V. 2002, *ApJ*, 567, L119
- Faber, S. M., & Jackson, R. E. 1976, *ApJ*, 204, 668



- Farrarese, L., & Merritt, D. 2000, *ApJ*, 539, L9
- Gebhardt, K., et al. 2000, *ApJ*, 539, L13
- Gebhardt, K., et al. 2003, *ApJ*, in press, astro-ph/0209483
- Genzel, R. et al. 1996, *ApJ*, 472, 153
- Gerhard, O., Kronawitter, A., Saglia, R. P., & Bender, R. 2001, *AJ*, 121, 1936
- Ghez, A., Klein, B. L., Morris, M., & Becklin, E. E. 1998, *ApJ*, 509, 678
- Haehnelt, M., & Kauffmann, G. 2000, *MNRAS*, 318, 35, astro-ph/0007369
- Ho, L. C. 1999, in *Observational Evidence for Black Holes in the Universe*, ed. S. K. Chakrabarti (Dordrecht: Kluwer), 157
- Hughes, S. A., & Blandford, R. D. 2002, astro-ph/0208484
- Jarvis, B. J., & Freeman, F. C. 1982, *ApJ*, 295, 324
- Jijina, J. 1999, PhD Thesis, Univ. Michigan
- Kauffmann, G., White, S.D.M., & Guiderdoni, B. 1993, *MNRAS*, 264, 201
- Kauffmann, G., & Haehnelt, M. G. 2000, *MNRAS*, 311, 576
- Kormendy, J. 2000, in *Galaxy Disks and Disk Galaxies* (astro-ph/0007401)
- Kormendy, J., & Richstone, D. 1995, *ARA&A*, 33, 581
- Kumar, P. 1999, *ApJ*, 519, 599
- Laor, A. 2001, *ApJ*, 553, 677
- Magorrian, J. et al. 1998, *AJ*, 115, 2285, astro-ph/9708072
- McLure, R. J., & Dunlop, J. S. 2002, *MNRAS*, 331, 795
- Menou, K., Haiman, Z., & Narayanan, V. K. 2001, *ApJ*, 558, 535
- Merritt, D., & Farrarese, L. 2001, *ApJ*, 547, 140, astro-ph/0008310
- Merritt, D., & Farrarese, L. 2001, *MNRAS*, 320, 30
- Misner, C. W., Thorne, K. S., & Wheeler, J. A. 1973, *Gravitation* (New York: Freeman)
- Myers, P. C., & Fuller, G. A. 1993, *ApJ*, 402, 635
- Ostriker, J. P. 2000, *Phys. Rev. Lett.*, 84, 5258, astro-ph/9912548

- Peebles, P.J.E. 1993, *Principles of Physical Cosmology* (Princeton: Princeton Univ. Press)
- Rees, M. J. 1984, *ARA&A*, 22, 471
- Richstone, D. O. 2002, in *Astrophysical Supercomputing using Particles*, IAU Symposium 208, eds. J. Makino & P. Hut, in press
- Richstone, D. O. et al. 1998, *Nature*, 395, A14
- Richtmyer, R. D. 1978, *Principles of Advanced Mathematical Physics* (New York: Springer-Verlag)
- Riffert, H. 2000, *ApJ*, 529, 119
- Shu, F. H. 1977, *ApJ*, 214, 488
- Shu, F. H. 1992, *Gas Dynamics* (Mill Valley: Univ. Science Books)
- Shu, F. H., Adams, F. C., & Lizano, S. 1987, *A R A & A*, 25, 23
- Silk, J., & Rees, M. J. 1998, *A & A*, 331, L1
- Somerville, R. S., & Primack, J. R. 1999, *MNRAS*, 310, 1087
- Sugerman, B., Summers, F. J., & Kamionkowski, M. 2000, *MNRAS*, 311, 762
- Terebey, S., Shu, F. H., & Cassen, P. 1984, *ApJ*, 286, 529
- Thorne, K. S. 1974, *ApJ*, 191, 507
- Thorne, K. S., Price, R. H., & MacDonald, D. A. 1986, *Black Holes: The Membrane Paradigm* (New Haven: Yale Univ. Press)
- Tremaine, S. et al. 2002, *ApJ*, 574, 740, astro-ph/0203468
- van der Marel, R. P. 1999, in *Galaxy Interactions at Low and High Redshift*, IAU Symposium 186, eds. J. E. Barnes & D. B. Sanders, p. 333
- Volonteri, M., Haardt, F., & Madau, P. 2003, *ApJ*, 582, 559
- White, S.D.M. 1979, *MNRAS*, 189, 831
- White, S.D.M. 1996, in *Cosmology and Large Scale Structure Les Houches LX*, eds. R. Schaeffer, J. Silk, M. Spiro, and J. Zinn-Justin (Elsevier), p. 349
- White, S.D.M., & Rees, M. J. 1978, *MNRAS*, 183, 341
- Wechsler, R. H., Bullock, J. S., Primack, J. R., Kravtsov, A. V., & Dekel, A. 2002, *ApJ*, 568, 52
- Wyse, R.F.G., & Gilmore, G. 1992, *AJ*, 104, 144

Yu, Q., & Tremaine, S. 2002, MNRAS, 335, 965

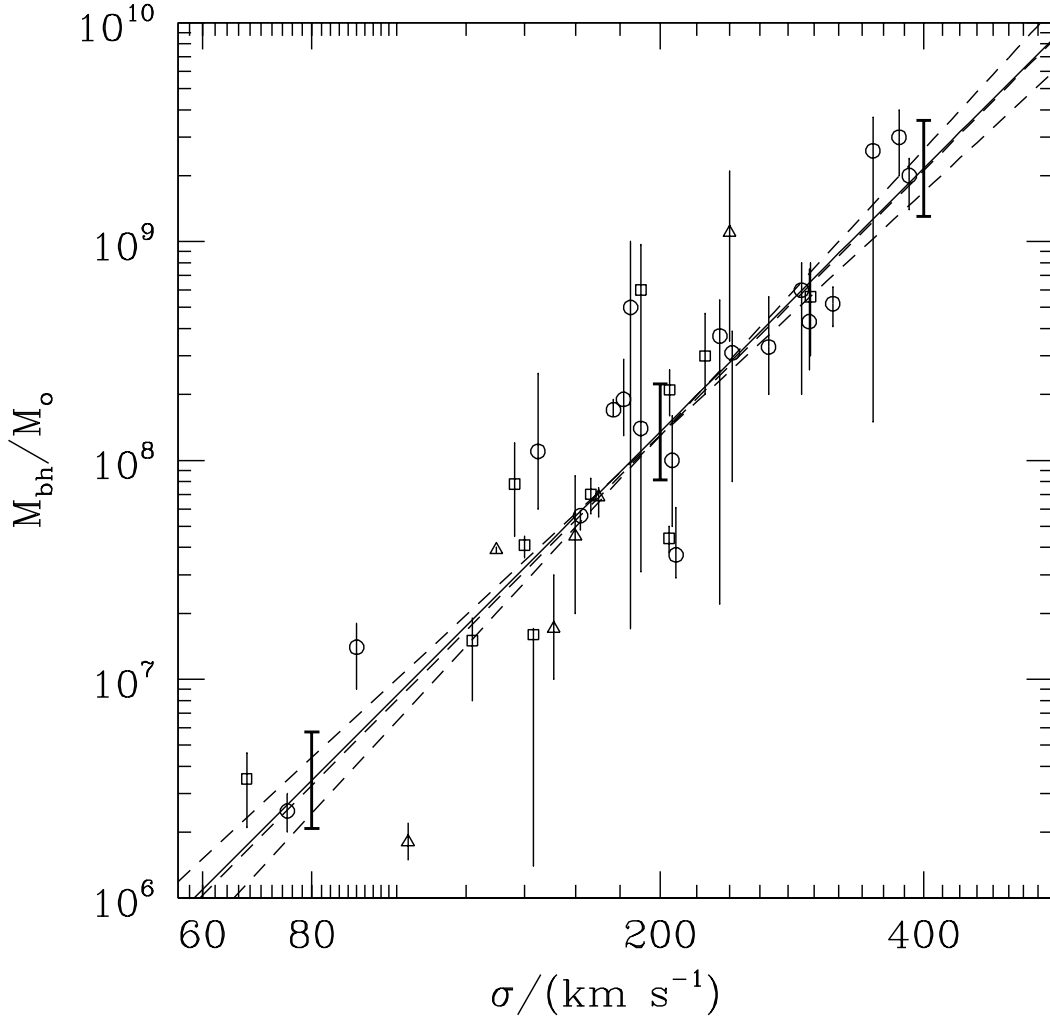


Fig. 1.— The correlation between black hole mass  $M_{\text{bh}}$  and velocity dispersion  $\sigma$  of the host galaxy. The data points (adapted from Gebhardt et al. 2003) represent the observed correlation for ellipticals (circles), S0 galaxies (squares), and spirals (triangles). The solid curve shows the theoretical result of this paper (using equation [22] with  $\mathcal{F}_A = 1.35$ ). The dashed curves show the observational fit advocated by Tremaine et al. (2002); curves are shown for the best estimate of the index  $\gamma = 4.02$  and for the maximum/minimum values  $\gamma = 4.02 \pm 0.32$ . The bold-faced error bar symbols show the level of scatter that would result if the initial rotation rate  $\Omega$  follows the same distribution as that of the spin parameter  $\lambda$  for galactic halos.

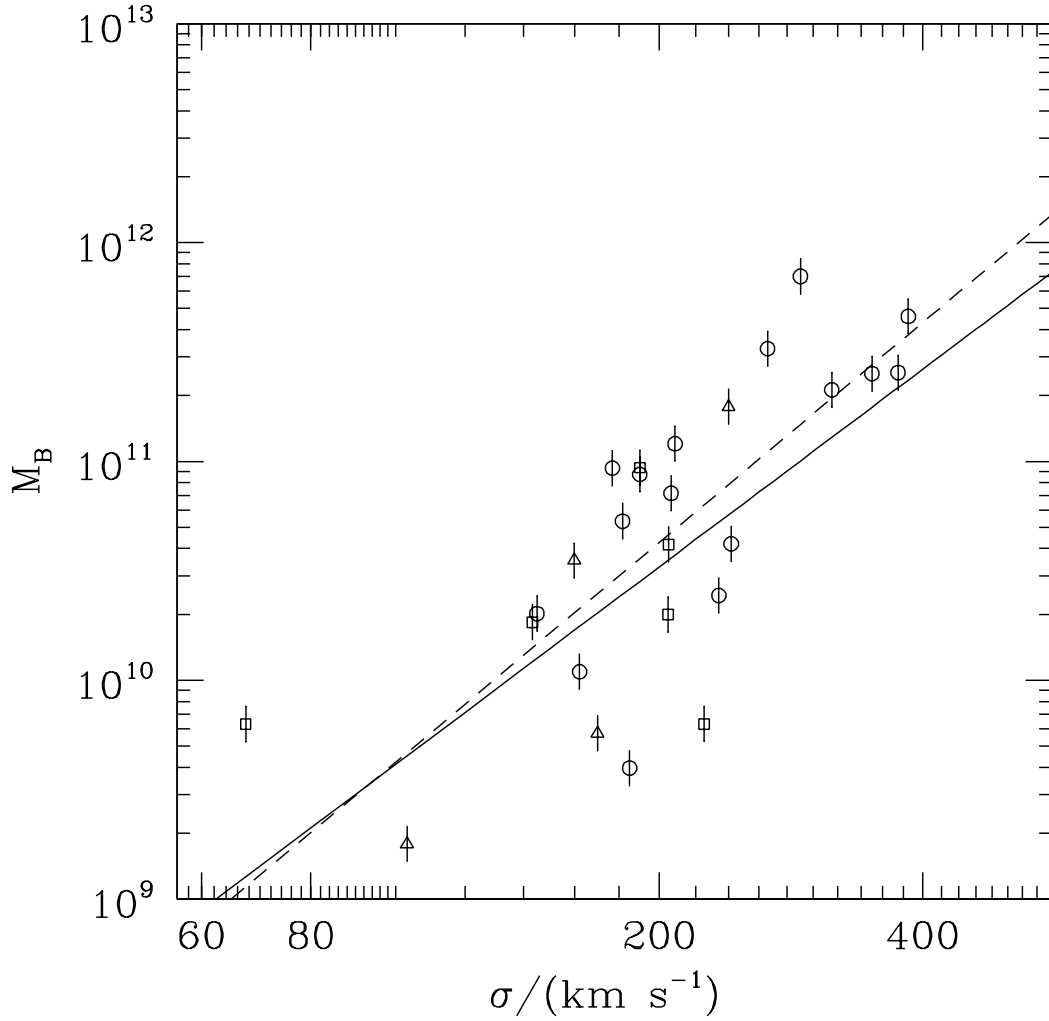


Fig. 2.— The correlation between bulge mass scale  $M_B$  and velocity dispersion  $\sigma$  of the host galaxy. The data points (adapted from Gebhardt et al. 2003) represent the observed correlation for ellipticals (circles), S0 galaxies (squares), and spirals (triangles). The error bars correspond to 20 percent uncertainties in the bulge mass estimates. The solid curve shows the theoretical mass scale predicted by the infall-collapse model of this paper (using equation [23] with  $\mathcal{F}_B = \pi/2$  and  $\mathcal{F}_{DM} = 1$ ). The dashed curve shows an unweighted least squares fit to the data.

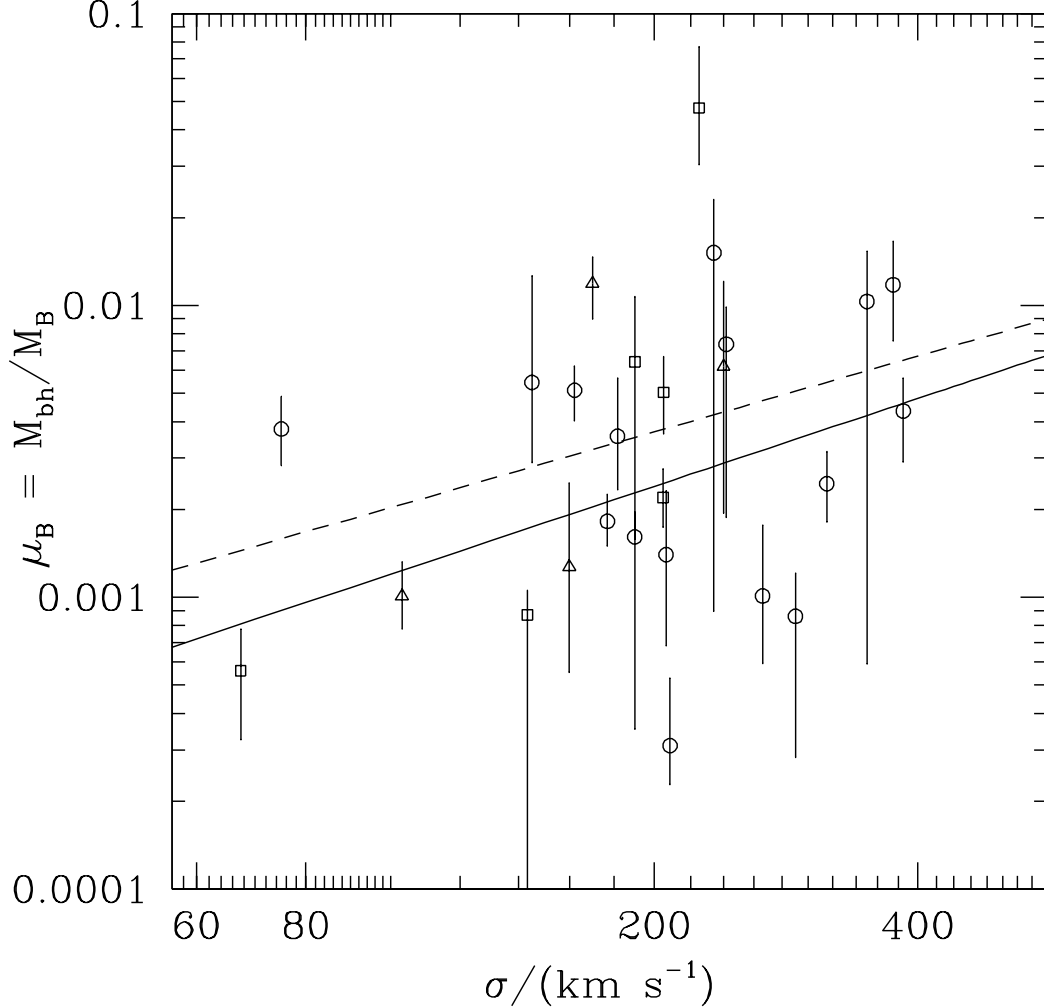


Fig. 3.— The ratio  $\mu_B$  of black hole mass  $M_{\text{bh}}$  to bulge mass scale  $M_B$  plotted as a function of the velocity dispersion  $\sigma$  of the host galaxy. The solid curve shows the prediction of equation [24], where we assume that the simple dynamical mass scale  $M_B$  from the collapse model can be identified with the bulge mass. The data points (adapted from Gebhardt et al. 2003) exhibit considerable scatter, but the least squares fit (shown as by the dashed curve with slope 0.86) is in reasonable agreement with theoretical expectations; the various symbols represent ellipticals (circles), S0 galaxies (squares), and spirals (triangles). The error bars are determined by the quadrature sum of the error bars shown in Figures 1 and 2.

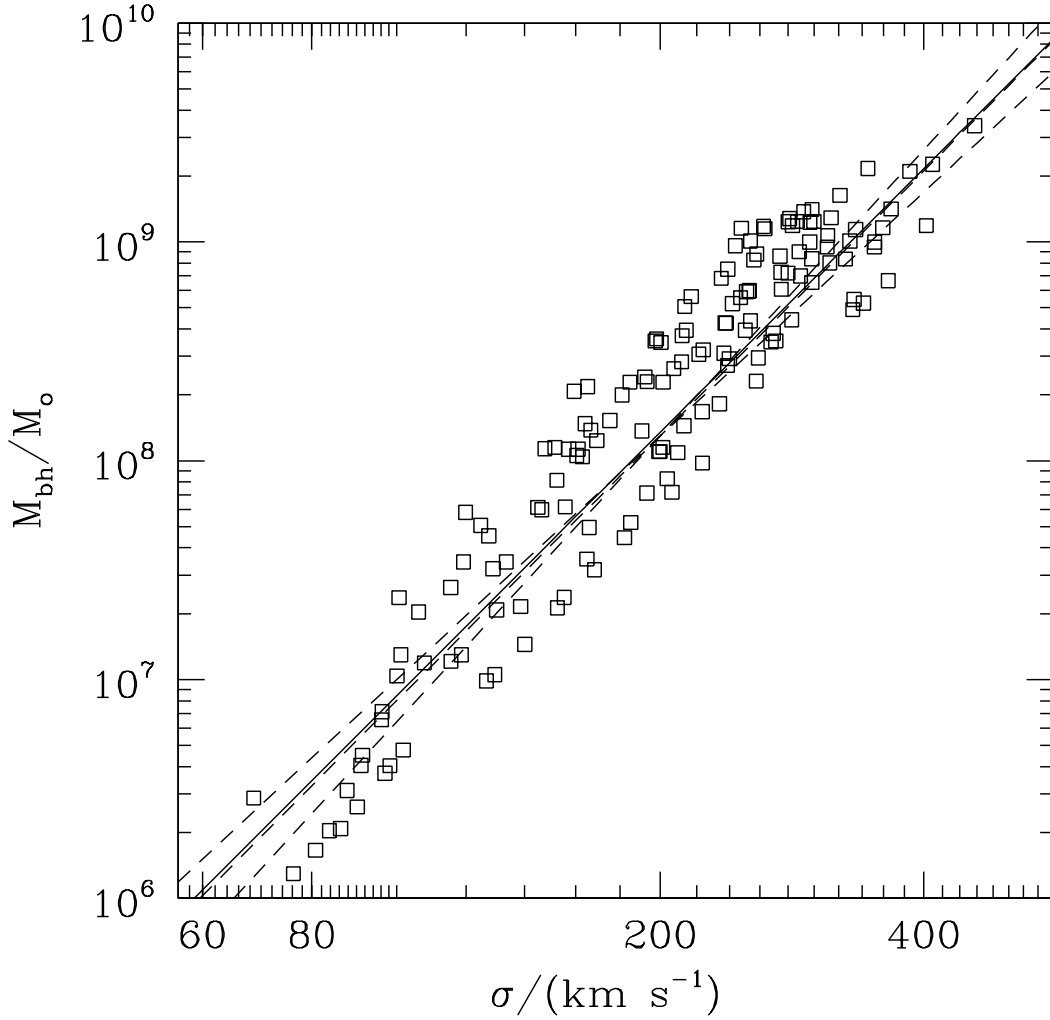


Fig. 4.— An illustration of the correlation between black hole mass  $M_{\text{bh}}$  and velocity dispersion  $\sigma$  being preserved under the action of mergers. The result of each numerical experiment is shown as an open square. The lines (for reference) are the same as those in Figure 1. The numerical experiments begin with  $N = 2 - 6$  smaller units, which are merged according to the rules of §3.5.